



Femtosecond laser ablated durable superhydrophobic PTFE films with micro-through-holes for oil/water separation: Separating oil from water and corrosive solutions



Jiale Yong^a, Yao Fang^a, Feng Chen^{a,*}, Jinglan Huo^a, Qing Yang^{b,*}, Hao Bian^a, Guangqing Du^a, Xun Hou^a

^a Department of Electronic Science and Technology, State Key Laboratory for Manufacturing System Engineering and Key Laboratory of Photonics Technology for Information of Shaanxi Province, School of Electronics & Information Engineering, Xi'an Jiaotong University, Xi'an, 710049, PR China
^b School of Mechanical Engineering, Xi'an Jiaotong University, Xi'an, 710049, PR China

ARTICLE INFO

Article history:

Received 6 May 2016

Received in revised form 16 June 2016

Accepted 12 July 2016

Available online 15 July 2016

Keywords:

Oil/water separation

Superhydrophobic

Femtosecond laser

Durability

PTFE

ABSTRACT

Separating the mixture of water and oil by the superhydrophobic porous materials has attracted increasing research interests; however, the surface microstructures and chemical composition of those materials are easily destroyed in a harsh environment, resulting in materials losing the superhydrophobicity as well as the oil/water separation function. In this paper, a kind of rough microstructures was formed on polytetrafluoroethylene (PTFE) sheet by femtosecond laser treatment. The rough surfaces showed durable superhydrophobicity and ultralow water adhesion even after storing in various harsh environment for a long time, including strong acid, strong alkali, and high temperature. A micro-through-holes array was further generated on the rough superhydrophobic PTFE film by a subsequent mechanical drilling process. The resultant sample was successfully applied in the field of oil/water separation due to the inverse superhydrophobicity and superoleophilicity. The designed separation system is also very efficient to separate the mixtures of oil and corrosive acid/alkali solutions, exhibiting the strong potential for practical application.

© 2016 Published by Elsevier B.V.

1. Introduction

With the global energy demand growing, oil spill accidents and industrial oily sewage discharges occur frequently [1–4]. Impressive examples such as the Gulf of Mexico oil spill [5]. This accident occurred in 2010 and resulted in 210 million gallons of oil being released on ocean surface. This accident not only caused huge economic loss, but also threatened the ecological system. With the toxic compounds (e.g., hydrogen sulfide, methylbenzene, aromatic hydrocarbons) in oil leaking into water, those toxic compounds quickly entered the food chain, hurting from lower algae to higher mammals for a long time. To avoid the above-mentioned disaster, oil/water separation technology has become an increasingly important topic for protecting environment and reducing economic loss [1,2,6–13]. Recently, superhydrophobic-superoleophilic or superoleophobic-superhydrophilic meshes or

porous materials have attracted much interests in the oil/water separation application due to the different interface effects of water and oil [14–21]. For example, Jiang et al. first used Teflon coated rough metal mesh to separate the mixture of oil and water [22]. The prepared mesh performed simultaneous superhydrophobicity and superoleophilicity; that is, a water droplet maintained a sphere shape on such mesh and could easily roll off, while oil droplet spread out quickly and permeated through the mesh, endowing the metal mesh with the ability of separating the oil/water mixtures. Sun et al. coated a layer of graphene oxide (GO) on a stainless steel wire mesh, and subsequent irradiated the mesh by O₂ plasma from the back side [23]. The GO-coated mesh exhibited underwater superoleophilicity and could separate the mixture of bean oil and water that imitated culinary sewage. Lai et al. used a one-step hydrothermal method to construct a superhydrophobic TiO₂ particles coated cotton fabric, which was highly efficient in oil/water separation because of its large contrast between oil and water wettability [24]. Pan et al. prepared a superhydrophobic/superoleophilic sponge by a solution-immersion process [25]. The oils and organic solvents on the water surface could be successfully removed and collected by the sponge. Based on the skeletons

* Corresponding authors.

E-mail addresses: chenfeng@mail.xjtu.edu.cn (F. Chen), haobian@mail.xjtu.edu.cn (H. Bian).

such as metal mesh, fabric and sponge, various superhydrophobic or superoleophobic materials were developed to efficiently separate the mixtures of water and oil [26–30]. However, most reported materials with super-wettability have poor durability. They will easily lose their oil/water separation function in harsh environments including strong acid or alkali corrosion, high temperature, friction and so on. Therefore, endowing the superhydrophobic or superoleophobic materials with stability is very important to extend the lifetime of the designed separation devices in practical application [31–33].

Polytetrafluoroethylene (PTFE) material is widely applied in the industrial field and our daily life for low cost, chemical inertness and environmental stability [34]. PTFE can hold original surface morphology and chemical composition even after storing in a harsh environment for a long time, such as strong acid/alkali solution, extreme temperature (-180°C – 250°C), organic solvents. Because of its low surface free energy and intrinsic hydrophobicity, stable superhydrophobicity can be directly obtained by designing micro/nanoscale structures on PTFE surface. Therefore, PTFE is considered to be a promising candidate for designing porous superhydrophobic membrane for oil/water separation application. The excellent stability is the advantage of PTFE material, but this property also brings difficulty to build rough microstructures on PTFE surfaces when we want to achieve superhydrophobicity through many common methods, such as chemical etching, self-assembly, thermal annealing, template method [35,36]. Recently, femtosecond laser microfabrication has been applied to obtain superhydrophobic and superoleophobic microstructures [37–43]. Micro/nanoscale rough structures can be directly formed by femtosecond laser ablation process on various materials including semiconductor, metals, ceramics, and glasses [38,44–47]. Likewise, the materials with anti-corrosion, high melting point, hardness or brittleness can also be ablated by femtosecond laser.

Here, we report the formation of rough microstructures on PTFE surface and realize durable superhydrophobicity by a simple femtosecond laser treatment. The sample maintained its superhydrophobicity even after suffering from the harsh environment storage for a long time. Furthermore, a drill process was implemented from the back side of the rough PTFE sheet to make micro-through-holes. The microholes array structured rough PTFE sheet repelled water, while oil could quickly penetrate through the resultant membrane. The as-prepared porous superhydrophobic film was successfully applied in the field of oil/water separation for the inverse superhydrophobicity and superoleophilicity.

2. Experimental section

2.1. Femtosecond laser ablation

PTFE sheet with the thickness of 0.3 mm was initially fixed on a platform whose movement was controlled by computer program. Then the sample was irradiated by the femtosecond laser beam coming from a Ti:sapphire laser system (Libra-usp-he, Coherent, America), as shown in Fig. 1a. The laser pulse duration, center wavelength, and repetition rate are 50 fs, 800 nm, and 1 kHz, respectively. The typical line-by-line scanning process was used, which referred to our previous work [43,48–50]. The used laser power was held constant at 20 mW. The laser beam was focused by an objective lens ($\times 20$, NA = 0.40, Nikon, Japan) on the sample surface to a spot diameter of about 10 μm . The scanning speed and the shift of adjacent laser scanning lines were adjusted by the movement of the mechanical platform.

2.2. Generating microholes array structure

To generate micro-through-holes array structure on the laser ablated PTFE sheet, a mini drill was used, which was fixed in a homemade mechanical system. The diameter of the drill bit was 0.3 mm. The drill bit was controlled to close and pass through the laser ablated PTFE sheet from the back side with the speed of 0.5 mm/s, resulting in a series of microscale open holes (Fig. 1b). By the aid of pre-designed program, uniform microholes array structure could even be fabricated.

2.3. Oil-water separation

The microholes array structured superhydrophobic PTFE sheet was sandwiched between two glass tubes (diameter = 30 mm), acting as a separating membrane (Fig. 1c). The glass tube was tilted 25° – 30° . After pouring the mixture of oil (petroleum ether) and water into the upper tube, the designed separation system started working. For the clearer observation, the used water and oil were dyed by methylene blue and Oil Red O, respectively. The strong acid ($\text{pH} \approx 1$) and strong alkali ($\text{pH} \approx 13$) were hydrochloric acid and potassium hydroxide solutions.

2.4. Characterization

The microtopography of the PTFE surface ablated by femtosecond laser was obtained using a Quanta 250 FEG scanning electron microscope (SEM, FEI, America). Deionized water and petroleum ether were used to investigate the wettabilities of both water and oil droplets on the as-prepared substrate. The contact angle (CA) and sliding angle (SA) were measured by a JC2000D contact-angle system (Powereach, China). The acid solution and alkali solution were obtained by diluting hydrochloric acid and potassium hydroxide with deionized water, respectively. pH value was monitored using a CT-6023 pH meter (Kedida, China). For the oil/water separation test, the separation efficiency was qualitatively analyzed with the aid of a DS-Fi2 optical microscope (Nikon, Japan).

3. Results and discussion

Fig. 2a–c shows the textured topography of the femtosecond laser ablated PTFE surface. The scanning speed and the shift of adjacent laser scanning lines were set at 5 mm/s and 5 μm , respectively. Large numbers of pores and protrusions were generated during the laser ablation process. The size of the protrusions is from 300 nm to 2 μm . Water droplet can maintain a sphere shape on the rough substrate, as shown in Fig. 2d and e. The static CA of water droplet reaches up to $155.5^{\circ} \pm 1.5^{\circ}$, indicating that the laser induced rough surfaces perform superhydrophobicity without any chemical modification. The combination of the intrinsic hydrophobicity and the rough microstructures play a very important role in forming superhydrophobicity on PTFE material [51,52].

The laser ablated PTFE surface has not only superhydrophobicity but also ultralow adhesion to a water droplet. Fig. 3a displays the rolling process of a water droplet on the superhydrophobic sample (Movie S1, Supporting information). The ultimate tilt angle of substrate when the droplet started to roll was only 2.5° ; that is, the SA is 2.5° . If a water droplet was released from a place above the as-prepared surface, the droplet would free fall and impact the substrate. As shown in Fig. 3b, the droplet initially deformed and contacted the sample surface as much as possible during the process of impact. Then, the shape of the droplet recovered to near sphere quickly. As a result, the droplet rebounded off and left the substrate. The droplet could bounce numerous times on the femtosecond laser ablated PTFE surface (Movie S2, Supporting information), confirming the ultralow adhesion of the

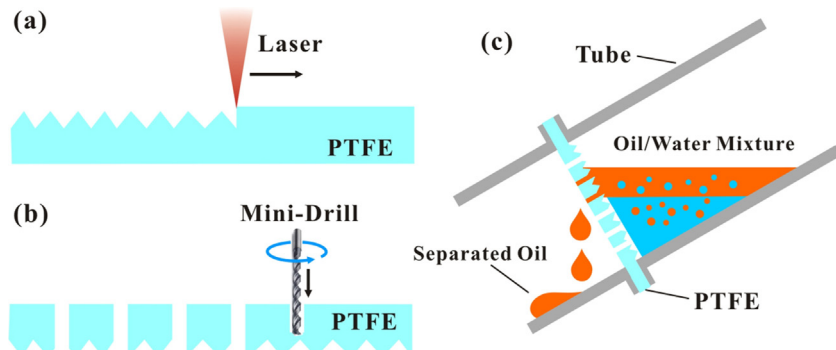


Fig. 1. Schematic illustration of the preparation of microholes array structured rough PTFE sheet and the designed oil/water separation device. (a) Femtosecond laser ablating PTFE surface. (b) Generating micro-through-holes array using a mini drill. (c) Oil/water separation device.

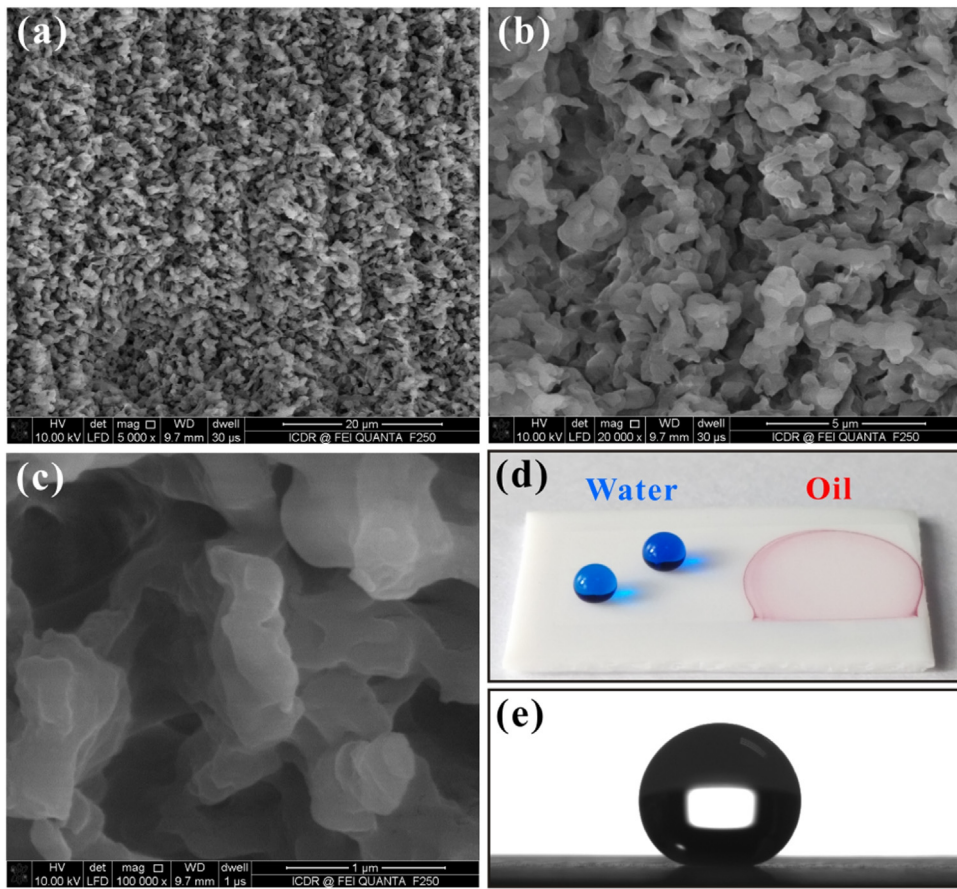


Fig. 2. (a–c) SEM images of the PTFE surface after femtosecond laser ablation. (d) Photo of two water droplets and one oil droplet on the rough substrate. (e) Contact angle measurement of a water droplet on the as-prepared surface.

superhydrophobic surface again. Superhydrophobicity ($CA \geq 150^\circ$) and ultralow adhesion ($SA \leq 10^\circ$) are the key distinct characteristic features of the Cassie-Baxter wetting state [53–55]. Water droplet on the sample surface only contacts the peak of the femtosecond laser induced rough microstructures. Air fills in the space of microstructures, resulting in a trapped air cushion between the rough surface microstructures and water droplet. The contact area between the droplet and the PTFE sheet is very small, endowing the femtosecond laser ablated PTFE surfaces with superhydrophobicity and low water adhesion. Interestingly, the oil wettability of the as-prepared surface is obviously different from the water wettability. It was found that the rough PTFE surface exhibited amazing superoleophilicity (Fig. 2d). If an oil droplet was dripped on the

substrate, the oil droplet would quickly spread out and fully wet the laser induced rough microstructures, as shown in Fig. 3c and Movie S3 (Supporting information). The flat untreated PTFE surface shows intrinsic hydrophobicity and oleophilicity, with CA of 111.5° to a water droplet and 10.4° to a petroleum ether droplet. Rough microstructure has an amplification effect on the wettability of solid surface, thereby resulting in the femtosecond laser ablated PTFE sheet exhibiting contrasting superhydrophobicity and superoleophilicity [56–59].

Laser scanning speed and scanning line interval are two crucial machining parameters. In our experiment, we tactfully combined those two parameters as a new one: average distance (AD) of laser pulse ablated points. AD was detailed in our previous work

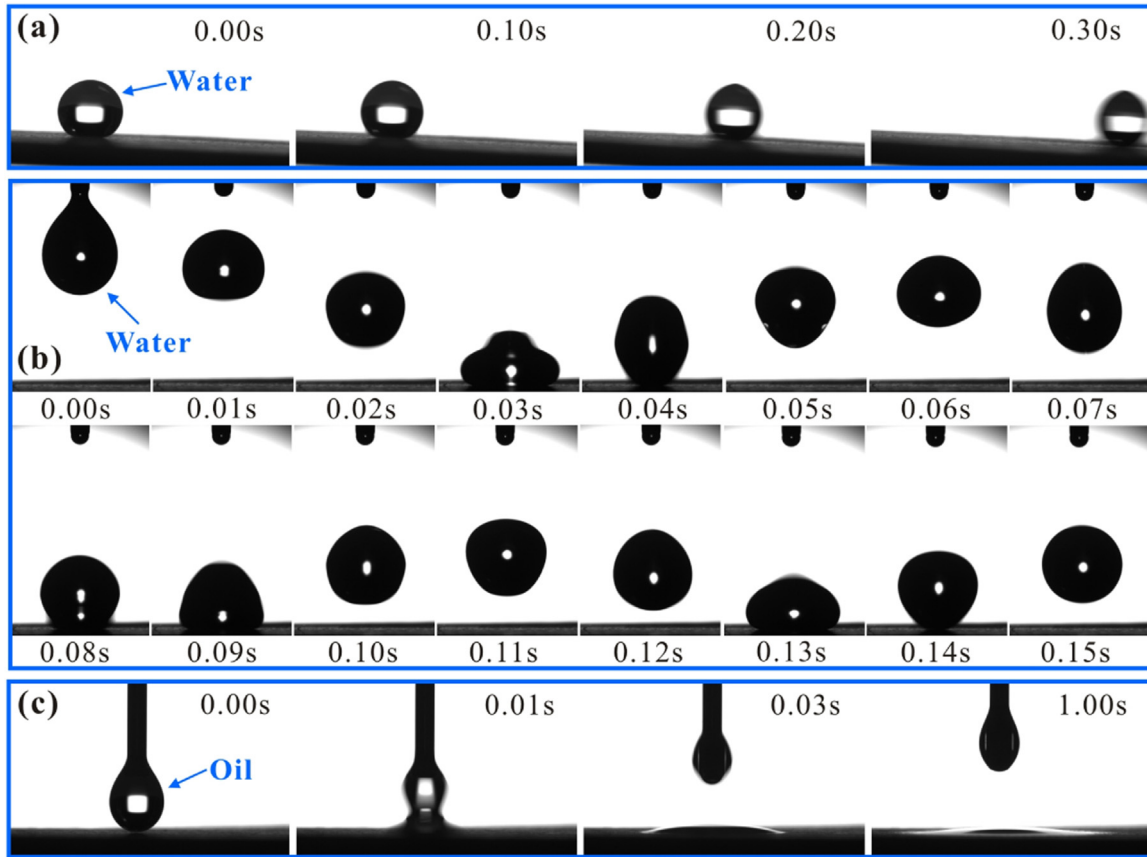


Fig. 3. (a) Water droplet rolling on the femtosecond laser ablated surface. (b) The droplet bounce behavior on the substrate. (c) Dripping an oil droplet on the rough PTFE surface.

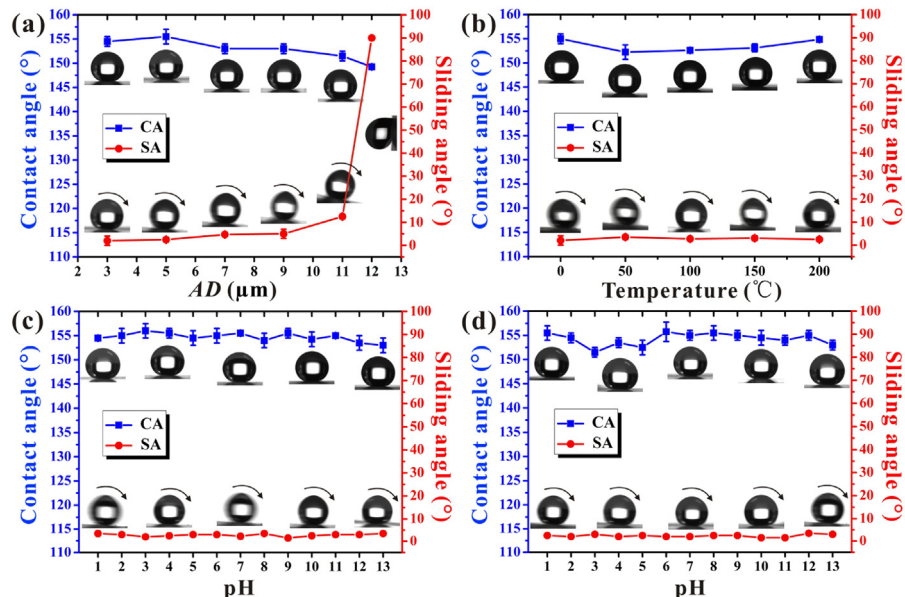


Fig. 4. Durability of the femtosecond laser induced superhydrophobic PTFE surfaces. (a) Wettability of the as-prepared samples fabricated at different machining parameters (AD). (b) Wettability of the as-prepared samples ($AD = 5 \mu\text{m}$) after storing at different temperature for one day. (c) Contact angle and sliding angle of a droplet with different pH values on the as-prepared surface ($AD = 5 \mu\text{m}$). (d) Wettability of the samples ($AD = 5 \mu\text{m}$) after immersing in water solutions with various pH for one day. The insets are the static shape and rolling snapshot of a water droplet on the corresponding samples.

[43,48,49]. Larger scanning speed and larger interval lead to a larger AD . Fig. 4a reveals the CA and SA values of a water droplet on the femtosecond laser ablated surfaces with different AD . As the AD increases from $3 \mu\text{m}$ to $11 \mu\text{m}$ and then to $12 \mu\text{m}$,

decreases from $154.5^\circ \pm 1^\circ$ to $151^\circ \pm 0.5^\circ$ and then to $149.3^\circ \pm 0.3^\circ$. On the contrary, the SA slowly grows from $2^\circ \pm 1^\circ$ to $5^\circ \pm 1^\circ$ when the AD changes from $3 \mu\text{m}$ to $9 \mu\text{m}$. These small SA values demonstrate the ultralow water adhesion of as-prepared samples. With

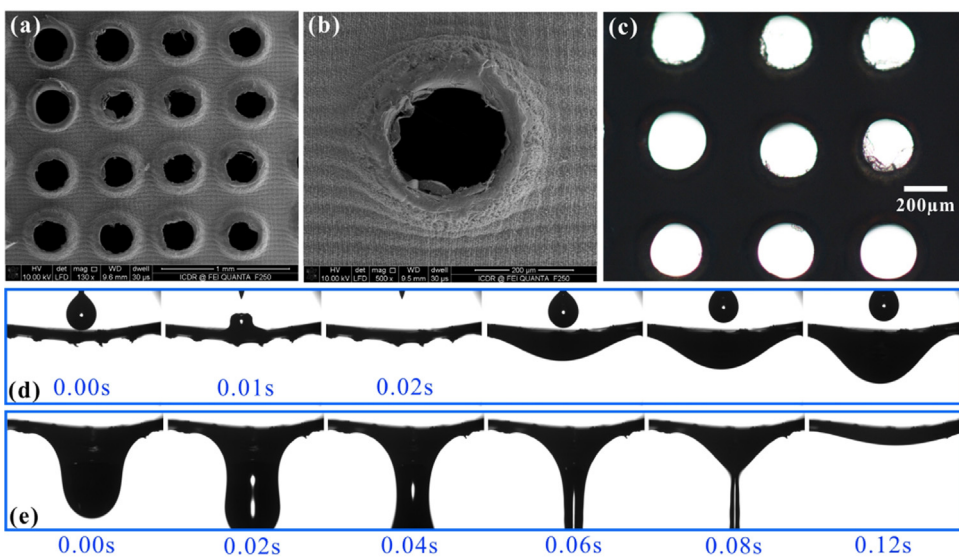


Fig. 5. (a, b) SEM images of the microholes array structured PTFE sheet. (c) Optical microscope photograph of the resultant surface. (d, e) Process of the oil droplet penetrating through the resultant PTFE film.

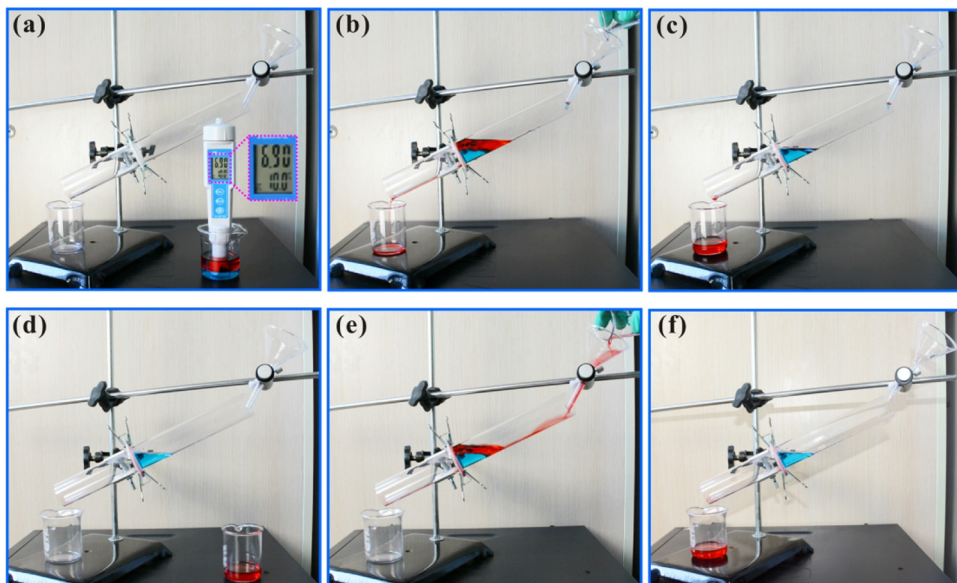


Fig. 6. Separating the mixture of oil (red) and water (blue) using the microholes array structured superhydrophobic PTFE sheet. (a–c) Pouring the mixture into the upper tube of the separation system. (d–f) Re-activating the oil/water separation process by introducing another newly oil into the upper tube. (For interpretation of the references to color in this figure legend, the reader is referred to the web version of this article.)

AD continuing increasing, SA has a significant rise. The SA can even reach up to 90° at $AD = 12 \mu\text{m}$; that is, a droplet adheres on the surface even when the sample is stood up. At small AD , the adjacent scanning lines were overlapped. A uniform rough microstructure was formed (Fig. 2a, b), which endowed the PTFE surface with ultralow adhesion. Whereas, the PTFE surface could not be fully ablated by femtosecond laser pulses if the AD was large enough to make the adjacent scanning lines independent with each other. Some non-ablated areas appeared between laser pulse irradiated rough craters, providing high adhesive force to water droplet. It was found that the ultralow adhesive superhydrophobicity can be obtained in a wide parameter range ($AD < 11 \mu\text{m}$).

The ultralow adhesive superhydrophobicity of the femtosecond laser induced PTFE surfaces is very stable. As shown in Fig. 4b, the water CA/SA does not show a significant change even after stor-

ing the samples ($AD = 5 \mu\text{m}$) at different temperature (0°C – 200°C) for one day. In addition, the resultant sample also maintains superhydrophobicity and ultralow adhesion for corrosive strong acid/alkaline solutions besides regular water. Fig. 4c shows the CA/SA results of a water droplet with different pH values on the as-prepared surface. All the CAs are above 150° while all the SA values are less than 10° as the pH changes from 1 to 13, exhibiting remarkable repellency towards acid/alkaline solutions. After the as-prepared samples ($AD = 5 \mu\text{m}$) being immersed in the water solutions with different pH for one day, respectively, no significant degradation of the ultralow adhesive superhydrophobicity of the resultant samples occurred (Fig. 4d). The durability is caused by the intrinsic chemical inertness of PTFE material and the femtosecond laser induced rough microstructures. The former endows the sample with an extremely slow damage process of the surface

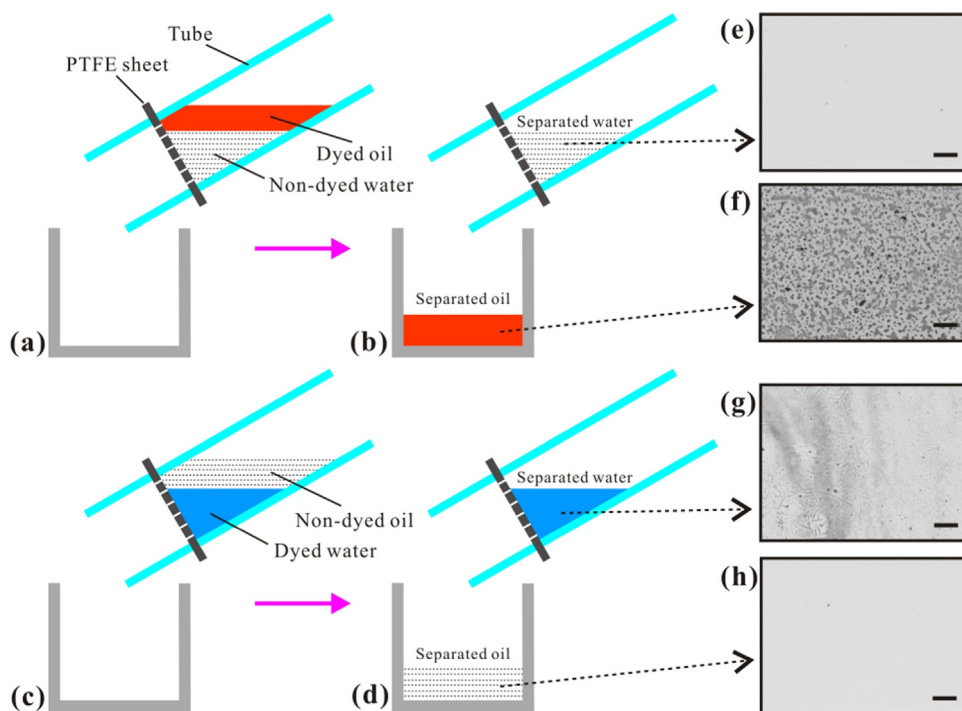


Fig. 7. Efficiency analysis of the designed oil/water separation system by an optical microscope. Scale bars: 50 μm .

chemical composition and topography, while the latter can amplify the above-mentioned effect because the rough microstructures significantly reduce the factual contact area between the PTFE and the corrosive liquid. The excellent durability makes the resultant superhydrophobic PTFE material be applied more widely and more flexibly, especially in the harsh environment or the chemical and biological field.

By combining the femtosecond laser ablation and the subsequent mechanical drilling process, a microholes array structured superhydrophobic PTFE sheet was fabricated, as shown in Fig. 5a, b. The sample surface is fully covered by rough microstructures for the laser ablation. In addition, there is an ordered open microholes array on its surface. The size of the holes is 240–280 μm . It is worth noting that the diameter of the microholes is smaller than that of the drill bit (300 μm). It may be that extrusion and stretch effects also occurred during the drilling process. When the sample was observed by an optical microscopy, it could be seen that the back-light penetrated through the microholes, whereas the rest region looked very dark (Fig. 5c). This result demonstrates that the drill-induced microholes are open, so the resultant superhydrophobic PTFE sheet will have a similar function as the rough metal mesh [60–62]. When an oil droplet was placed onto the microholes array structured superhydrophobic PTFE sheet, the oil would spread quickly on the sample surface within only 0.02 s, showing remarkable superoleophilicity (Fig. 5d). With the oil amount increasing, the oil would penetrate through the PTFE sheet and eventually drip down due to superoleophilicity and perforated micropores of the as-prepared substrate (Fig. 5d, e, Movie S4, Supporting information).

The superhydrophobic PTFE sheet with microholes array structure can be used to separate the mixture of water and oil. As shown in Fig. 6a, the resultant sheet was acted as a separating membrane and was sandwiched between two glass tubes. After pouring the mixture of oil (petroleum ether) and water into the upper tube, only the oil passed through the PTFE sheet and dripped into the beaker below, whereas the water was prevented and retained in the upper tube (Fig. 6b, c, Movie S5, Supporting information). The

used water is neutral with pH of about 6.9. The separation process was driven by the gravity, without any external applied force. The result demonstrates that the microholes array structured superhydrophobic PTFE sheet can be functioned as an oil/water separating membrane. The remarkable separation ability is caused by the diametrically opposite wettability for water and oil. It is worth noting that the treatment of the PTFE surface by femtosecond laser was essential to allow the oil and water to be separated. The femtosecond laser induced rough microstructures can enhance the intrinsic wettability of PTFE sheet, endowing the treated surface with simultaneous superhydrophobicity and superoleophilicity. The superhydrophobicity prevents water from wetting the laser-treated rough PTFE sheet drilled with an array of microholes, while the superoleophilicity makes the oil rapidly wet and pass through the microholes. If the microholes structured flat PTFE sheet without previous femtosecond laser ablation was used in the separation experiment, both water and oil could percolate through the sheet after the mixture being poured onto the separation system.

When the oil was separated out, the separation process would stop and quiet down at last. Interestingly, if some oil were poured into the upper tube just after an oil/water separation cycle had finished, the newly introduced oil would pass through the PTFE sheet again, while the water still stayed in the upper tube (Fig. 6d–f, Movie S6, Supporting information). The result reveals that the separation process can be restarted instantly if another new mixture is added into the designed device. Therefore, the separation process can be cycled many times, and the separation device can be used continuously.

The separation efficiency of the microholes array structured superhydrophobic PTFE sheet was investigated by the aid of an optical microscope. Firstly, we performed the separation experiment using the mixture of dyed oil and non-dyed water (Fig. 7a). When the separation process was finished (Fig. 7b), liquid droplet samples were taken from the separated oil and separated water, respectively, and placed on the glass slides. After the liquid being evaporated, the corresponding glass slides were observed with an

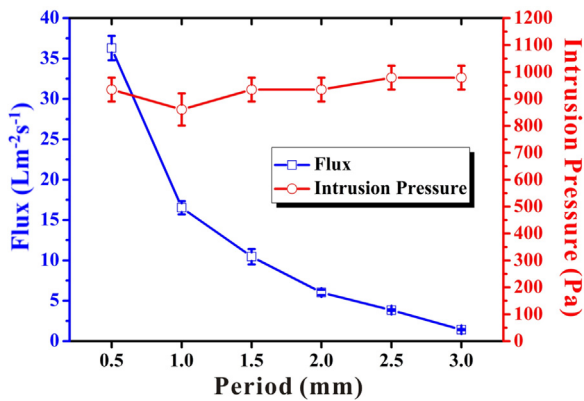


Fig. 8. Influence of the period of the microholes array on oil flux and intrusion pressure of the designed separation system.

optical microscope. The results are shown in Fig. 7e and f, respectively. It can be clearly seen that there are many textured stains on the glass where the separated oil droplet was put on (Fig. 7f). The rough texture was resulted from the dye (Oil Red O). However, there are no similar stains in the image of Fig. 7e. Next, we used the mixture of non-dyed oil and dyed water to repeat the above-mentioned process. The image of the separated water is shown in Fig. 7g while the image of the separated oil is shown in Fig. 7h. The glass slide in Fig. 7h is very clean, whereas there are many microscale vestiges on the glass where the separated water droplet was put on. The vestiges were resulted from the methylene blue dye. By comparing the Fig. 7e and f, we can draw a conclusion that there is almost none oil in the separated water. Similarly, by comparing the Fig. 7g and h, we can draw a conclusion that there is almost none water in the separated oil. Therefore, the device based on the microholes array structured superhydrophobic PTFE sheet performs very high separation efficiency.

The period or the space of the micro-through-holes array has vital influence on the oil flux of the designed separation system. The flux was calculated by measuring the time of an oil column with the height of 10 cm passing through the resultant sheets.

Fig. 8 reveals the variation of oil flux with the period. The oil flux decreases quickly with the period increasing due to a decrease of the density of the microholes. When the period is 0.5 mm (that is, the density of the microholes equals 400 cm^{-2}), the oil flux can reach up to $36.9 \text{ L m}^{-2} \text{ s}^{-1}$. Besides the flux, the intrusion pressure of water is another important performance of the designed separation device, which was measured by the maximum supporting height of a water column. Interestingly, for different period values, the intrusion pressures have almost no difference in the range of experimental errors (Fig. 8). This may be that the micro-through-holes are independent of each other, which is different with rough meshes and fabrics [8,17,63]. To obtain a maximum separation speed, a smaller period of the microholes array is better.

The as-prepared microholes array structured PTFE sheet shows superhydrophobicity, superoleophilicity, and chemical durability. It is also very efficient to separate the mixture of oil and strong acid/alkali solutions. Fig. 9a–c displays the separating ability of the superhydrophobic sheet for the corrosive oil/strong acid mixture. When the mixture of oil and HCl solution ($\text{pH} \approx 1$) was poured into the separation system, the red oil liquid could quickly pass through the PTFE sheet by the driving force of gravity (Movie S7, Supporting information). However, the blue water was prevented and remained in the upper tube for the superhydrophobicity. Using the same operational process, the corrosive mixture of oil and KOH solution ($\text{pH} \approx 13$) was also successfully separated (Fig. 9d–f, Movie S8, Supporting information). The chemical inertness of the PTFE material endows the laser ablated surface with durable superhydrophobicity. In addition, a liquid-infused porous interface was also spontaneously formed during the separation process since oil wetted and passed through the microholes. The oil-infused porous interface is generally very stable and has strong water-repellent ability because oil molecules (which are non-polar) strongly repel water molecules (which are polar) [64]. As a result, the designed separation system can work in various harsh environments, which will offer important opportunities in practical oil/water separation application.

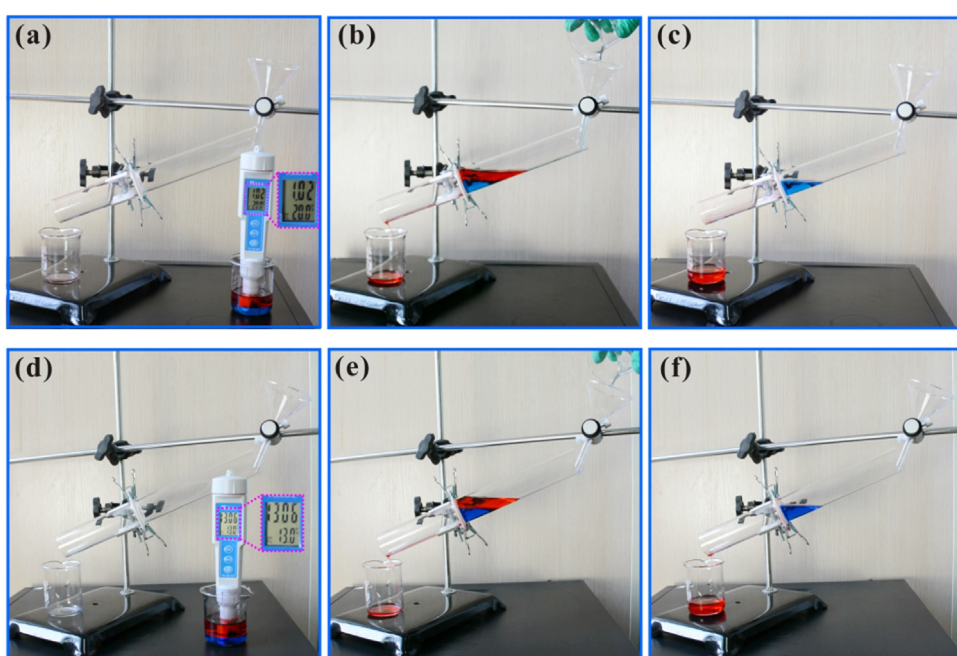


Fig. 9. Separation ability of the microholes array structured superhydrophobic PTFE sheet for the corrosive mixtures of oil and strong acid/alkali solutions.

4. Conclusions

In summary, durable superhydrophobicity and supereoleophilicity were achieved on the PTFE surface by a femtosecond laser ablation process. The CA of a water droplet on the laser irradiated substrate reached up to 155.5°, while the SA was only 2.5°. The as-prepared surface maintained its superhydrophobicity even after storing in various harsh environment for a long time, including strong acid, strong alkali, and high temperature. In addition, a micro-through-holes array was generated on the rough superhydrophobic PTFE sheet by subsequent mechanical drilling process. Oil droplet could spread out quickly and penetrate through the microholes array structured superhydrophobic PTFE sheet, whereas water was prevented and retained on the sample surface. Using the resultant sheet as the separation membrane, efficiently separating the mixtures of oil and corrosive acid/alkali solutions has been demonstrated. The as-prepared stable superhydrophobic sheets can work in various harsh environments, which have potential usage in practically solving the pollution problems caused by oily industrial wastewater and oil spills.

Acknowledgments

This work is supported by the National Science Foundation of China under the Grant nos. 61275008, 51335008 and 61475124, the Special-funded programme on national key scientific instruments and equipment development of China under the Grant no. 2012YQ12004706, the Collaborative Innovation Center of Suzhou Nano Science and Technology and the International Joint Research Center for Micro/Nano Manufacturing and Measurement Technologies. The SEM work was done at International Center for Dielectric Research (ICDR), Xi'an Jiaotong University.

Appendix A. Supplementary data

Supplementary data associated with this article can be found, in the online version, at <http://dx.doi.org/10.1016/j.apsusc.2016.07.075>.

References

- [1] B. Wang, W. Liang, Z. Guo, W. Liu, *Chem. Soc. Rev.* 44 (2015) 336–361.
- [2] Z. Xue, Y. Cao, N. Liu, L. Feng, L. Jiang, *J. Mater. Chem. A* 2 (2014) 2445–2460.
- [3] C.-F. Wang, F.-S. Tzeng, H.-G. Chen, C.-J. Chang, *Langmuir* 28 (2012) 10015–10019.
- [4] J.L. Yong, F. Chen, Q. Yang, H. Bian, G.Q. Du, C. Shan, J.L. Huo, Y. Fang, X. Hou, *Adv. Mater. Interfaces* 3 (2016) 1500650.
- [5] https://en.wikipedia.org/wiki/Deepwater_Horizon_oil_spill.
- [6] X. Gao, L.-P. Xu, Z. Xue, L. Feng, J. Peng, Y. Wen, S. Wang, X. Zhang, *Adv. Mater.* 26 (2014) 1771–1775.
- [7] M. Tao, L. Xue, F. Liu, L. Jiang, *Adv. Mater.* 26 (2014) 2943–2948.
- [8] K. He, H. Duan, G.Y. Chen, X. Liu, W. Yang, D. Wang, *ACS Nano* 9 (2015) 9188–9198.
- [9] K. Liu, J. Ju, Z. Xue, J. Ma, L. Feng, S. Gao, L. Jiang, *Nat. Commun.* 4 (2013) 2276.
- [10] R. Du, Z. Zheng, N. Mao, N. Zhang, W. Hu, J. Zhang, *Adv. Sci.* 2 (2015) 1400006.
- [11] Q. Liu, A.A. Patel, L. Liu, *ACS Appl. Mater. Interfaces* 6 (2014) 8996–9003.
- [12] C.-H. Xue, Y.-R. Li, J.-L. Hou, L. Zhang, J.-Z. Ma, *J. Mater. Chem. A* 3 (2015) 10248–10253.
- [13] B. Li, L. Wu, L. Li, S. Seeger, J. Zhang, A. Wang, *ACS Appl. Mater. Interfaces* 6 (2014) 11581–11588.
- [14] Z. Xue, S. Wang, L. Lin, L. Chen, M. Liu, L. Feng, L. Jiang, *Adv. Mater.* 23 (2011) 4270–4273.
- [15] A.K. Kota, G. Kwon, W. Choi, J.M. Mabry, A. Tuteja, *Nat. Commun.* 3 (2012) 1025.
- [16] F. Zhang, W.B. Zhang, Z. Shi, D. Wang, J. Jin, L. Jiang, *Adv. Mater.* 25 (2013) 4192–4198.
- [17] Q. Wen, J. Di, L. Jiang, J. Yu, R. Xu, *Chem. Sci.* 4 (2013) 591–595.
- [18] J. Song, S. Huang, Y. Lu, X. Bu, J.E. Mates, A. Ghosh, R. Ganguly, C.J. Carmalt, I.P. Parkin, W. Xu, A. Megaridis, *ACS Appl. Mater. Interfaces* 6 (2014) 19858–19865.
- [19] J.Y. Huang, S.H. Li, M.Z. Ge, L.N. Wang, T.L. Xing, G.Q. Chen, X.F. Liu, S.S. Al-Deyab, K.Q. Zhang, T. Chen, Y.K. Lai, *J. Mater. Chem. A* 3 (2015) 2825–2832.
- [20] D. Ge, L. Yang, C. Wang, E. Lee, Y. Zhang, S. Yang, *Chem. Commun.* 51 (2015) 6149–6152.
- [21] S. Wang, X. Peng, L. Zhong, J. Tan, S. Jing, X. Cao, W. Chen, C. Liu, R. Sun, J. Mater. Chem. A 3 (2015) 8772–8781.
- [22] L. Feng, Z. Zhang, Z. Mai, Y. Ma, B. Liu, L. Jiang, D. Zhu, *Angew. Chem. Int. Ed.* 43 (2004) 2012–2014.
- [23] Y.-Q. Liu, Y.-L. Zhang, X.-Y. Fu, H.-B. Sun, *ACS Appl. Mater. Interfaces* 7 (2015) 20930–20936.
- [24] S. Li, J. Huang, M. Ge, C. Cao, S. Deng, S. Zhang, G. Chen, K. Zhang, S.S. Al-Deyab, Y. Lai, *Adv. Mater. Interfaces* 2 (2015) 1500220.
- [25] Q. Zhu, Q. Pan, F. Liu, *J. Phys. Chem. C* 115 (2011) 17464–17470.
- [26] Z. Cheng, H. Lai, Y. Du, K. Fu, N. Zhang, K. Sun, *ACS Appl. Mater. Interfaces* 5 (2013) 11363–11370.
- [27] Y. Liu, J. Ma, T. Wu, X. Wang, G. Huang, Y. Liu, H. Qiu, Y. Li, W. Wang, J. Gao, *ACS Appl. Mater. Interfaces* 5 (2013) 10018–10026.
- [28] A. Zhang, M. Chen, C. Du, H. Guo, H. Bai, L. Li, *ACS Appl. Mater. Interfaces* 5 (2013) 10201–10206.
- [29] Y. Gao, Y.S. Zhou, W. Xiong, M. Wang, L. Fan, H. Rabiee-Golgir, L. Jiang, W. Hou, X. Huang, L. Jiang, J.-F. Silvain, Y.F. Lu, *ACS Appl. Mater. Interfaces* 6 (2014) 5924–5929.
- [30] X. Zhao, L. Li, B. Li, J. Zhang, A. Wang, *J. Mater. Chem. A* 2 (2014) 18281–18287.
- [31] J. Li, L. Yan, H. Li, W. Li, F. Zha, Z. Lei, *J. Mater. Chem. A* 3 (2015) 14696–14702.
- [32] Y. Hou, Z. Wang, J. Guo, H. Shen, H. Zhang, N. Zhao, Y. Zhao, L. Chen, S. Liang, J. Jin, J. Xu, *J. Mater. Chem. A* 3 (2015) 23252–23260.
- [33] X. Zhou, Z. Zhang, X. Xu, F. Guo, X. Zhu, X. Men, B. Ge, *ACS Appl. Mater. Interfaces* 5 (2013) 7208–7214.
- [34] <https://en.wikipedia.org/wiki/Polytetrafluoroethylene>.
- [35] T. Darmanin, F. Guittard, *J. Mater. Chem. A* 2 (2014) 16319–16359.
- [36] P. Ragesh, V.A. Ganesh, S.V. Nair, A.S. Nair, *J. Mater. Chem. A* 2 (2014) 14773–14797.
- [37] J.L. Yong, F. Chen, Q. Yang, X. Hou, *Soft Matter* 11 (2015) 8897–8906.
- [38] F. Chen, D.S. Zhang, Q. Yang, J.L. Yong, G.Q. Du, J.H. Si, F. Yun, X. Hou, *ACS Appl. Mater. Interfaces* 5 (2013) 6777–6792.
- [39] H.-B. Jiang, Y.-L. Zhang, D.-D. Han, H. Xia, J. Feng, Q.-D. Chen, Z.-R. Hong, H.-B. Sun, *Adv. Funct. Mater.* 24 (2014) 4595–4602.
- [40] D.S. Zhang, F. Chen, Q. Yang, J.L. Yong, H. Bian, Y. Ou, J.H. Si, X.W. Meng, X. Hou, *ACS Appl. Mater. Interfaces* 4 (2012) 4905–4912.
- [41] J.L. Yong, Q. Yang, F. Chen, D.S. Zhang, U. Farooq, G.Q. Du, X. Hou, *J. Mater. Chem. A* 2 (2014) 5499–5507.
- [42] J.L. Yong, F. Chen, Q. Yang, D.S. Zhang, U. Farooq, G.Q. Du, X. Hou, *J. Mater. Chem. A* 2 (2014) 8790–8795.
- [43] J.L. Yong, F. Chen, Q. Yang, G.Q. Du, C. Shan, H. Bian, U. Farooq, X. Hou, *J. Mater. Chem. A* 3 (2015) 9379–9384.
- [44] A.Y. Vorobyev, C.L. Guo, *Laser Photonics Rev.* 7 (2013) 385–407.
- [45] K. Sugioka, Y. Cheng, *Appl. Phys. Rev.* 1 (2014) 041303.
- [46] S. Kawata, H.-B. Sun, T. Tanaka, K. Takada, *Nature* 412 (2001) 697–698.
- [47] J.L. Yong, F. Chen, Q. Yang, U. Farooq, X. Hou, *J. Mater. Chem. A* 3 (2015) 10703–10709.
- [48] J.L. Yong, F. Chen, Q. Yang, G.Q. Du, H. Bian, D.S. Zhang, J.H. Si, F. Yun, X. Hou, *ACS Appl. Mater. Interfaces* 5 (2013) 9382–9385.
- [49] J.L. Yong, F. Chen, Q. Yang, D.S. Zhang, H. Bian, G.Q. Du, J.H. Si, X.W. Meng, X. Hou, *Langmuir* 29 (2013) 3274–3279.
- [50] J.L. Yong, F. Chen, Q. Yang, D.S. Zhang, G.Q. Du, J.H. Si, F. Yun, X. Hou, *J. Phys. Chem. C* 117 (2013) 24907–24912.
- [51] F. Xia, L. Jiang, *Adv. Mater.* 20 (2008) 2842–2858.
- [52] K. Liu, L. Jiang, *Chem. Soc. Rev.* 39 (2010) 3240–3255.
- [53] L. Feng, S. Li, Y. Li, H. Li, L. Zhang, J. Zhai, Y. Song, B. Liu, L. Jiang, D. Zhu, *Adv. Mater.* 14 (2002) 1857–1860.
- [54] S. Wang, L. Jiang, *Adv. Mater.* 19 (2007) 3423–3424.
- [55] Y. Zheng, X. Gao, L. Jiang, *Soft Matter* 3 (2007) 178–182.
- [56] Z. Xue, M. Liu, L. Jiang, *J. Polym. Sci. B: Polym. Phys.* 50 (2012) 1209–1224.
- [57] Y. Tian, B. Su, L. Jiang, *Adv. Mater.* 26 (2014) 6872–6897.
- [58] L. Wen, Y. Tian, L. Jiang, *Angew. Chem. Int. Ed.* 54 (2015) 3387–3399.
- [59] J.L. Yong, F. Chen, Q. Yang, Y. Fang, J.L. Huo, X. You, *Chem. Commun.* 51 (2015) 9813–9816.
- [60] B. Cortese, D. Caschera, F. Federici, G.M. Ingo, G. Gigli, *J. Mater. Chem. A* 2 (2014) 6781–6789.
- [61] M.A. Gondal, M.S. Sadullah, M.A. Dastageer, G.H. McKinley, D. Panchanathan, K.K. Varanasi, *ACS Appl. Mater. Interfaces* 6 (2014) 13422–13429.
- [62] Y. Yu, H. Chen, Y. Liu, V. Craig, L.H. Li, Y. Chen, *Adv. Mater. Interfaces* 1 (2014) 1300002.
- [63] D. Tian, X. Zhang, Y. Tian, Y. Wu, X. Wang, J. Zhai, L. Jiang, *J. Mater. Chem.* 22 (2012) 19652–19657.
- [64] T.-K. Wong, S.H. Kang, S.K.Y. Tang, E.J. Smythe, B.D. Hatton, A. Grinthal, J. Aizenberg, *Nature* 477 (2011) 443–447.